

Towards Understanding Skyglow

A contribution to the discussion

by Dr Christopher J Baddiley BSc. M.Inst.P. Ch.Phys. FRAS
(The British Astronomical Association Campaign for Dark Skies)
and Tom Webster I.Eng. M.I.L.E. (Institution of Lighting Engineers)



British Astronomical Association
Campaign for Dark Skies

38 The Vineries
Colehill
Wimborne
Dorset
BH21 2PX



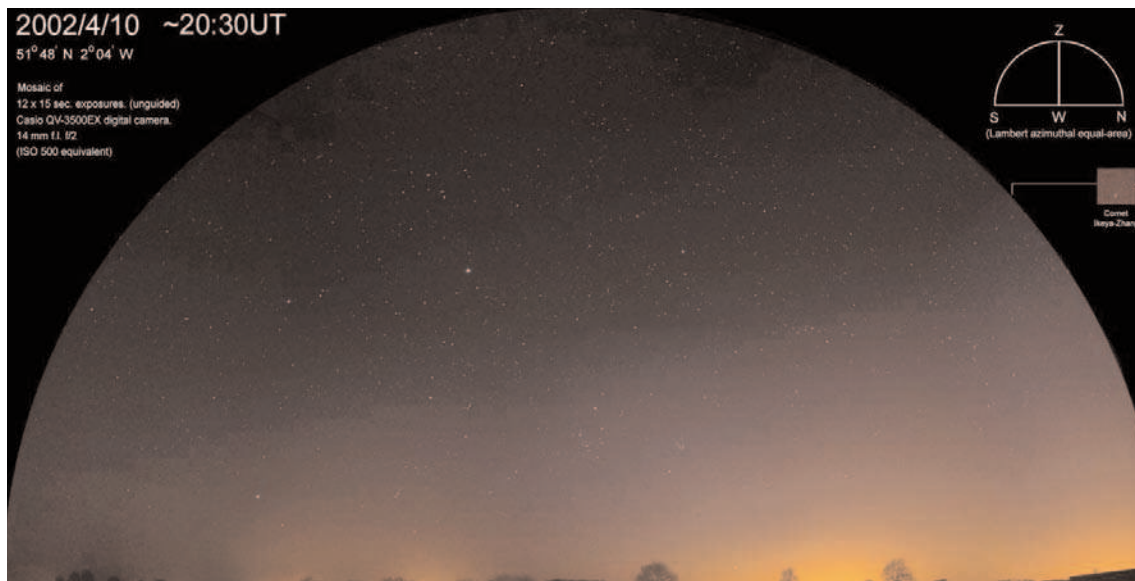
Institution of
Lighting Engineers

Regent House
Regent Place
Rugby
CV21 2 PN

The Institution of Lighting Engineers is pleased to publish this publication as a discussion document. However, pending further research the findings of the authors does not necessarily represent the views of the ILE.

Copyright for this document resides jointly with the ILE and the CfDS. Copying of any or all of the contents of this document should only be undertaken with the express authorisation of either organisation.

© CfDS/ILE October 2007



Cover image: A CCD composite slyglow image from the Cotswolds , by James Weightman

Towards Understanding Skyglow

Foreword	4
Skyglow in the UK	5
Skyglow: an executive summary	7
Skyglow photometry of night sky images in rural areas	8
Mathematical modelling of skyglow	10
The luminaires	10
Reflectivity	12
Luminaire upward light and reflection distributions	14
Atmospheric scattering	15
Scattering by air molecules	15
Scattering by air borne particles (aerosols)	16
Geometry	16
Scattering increment	17
The relative importance of ground reflected to direct light, and aerosol to molecular scattering	18
Output plots from the program	18
Accuracy of modelling	19
Rural skyglow dependence on luminaire types	20
Summary	22
Conclusions	23
Bibliography	24

Foreword

Stray light from our towns and cities is illuminating the sky over great distances and is eradicating our enjoyment of night skies. This stray light phenomenon is known as skyglow and although an awareness of the problem has been around for many years, the mechanism of skyglow, how it is created and what the key causative agents are, have not been fully appreciated. Now groundbreaking work by Dr. Chris Baddiley has increased our understanding, by developing a computer model of skyglow linked to industry standard luminaire photometry files and referencing it to measured skyglow. As a result, we can now understand the mechanism behind skyglow which, at last, gives us the rationale to successfully tackle this problem.

Tom Webster

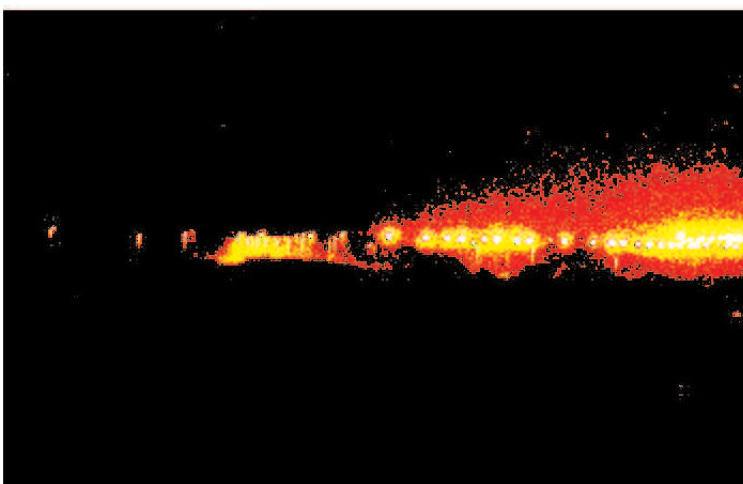
Skyglow in the UK

In 2003, the Campaign to Protect Rural England (CPRE) collaborated with the British Astronomical Association (BAA) Campaign for Dark Skies (CfDS) and launched their 'Night Blight' campaign. The campaign made use of data from the American National Oceanographic Atmospheric Administration Defence Meteorological Satellite Program (NOAA DMSP) for 1993 and 2001 to derive night light level maps for these years. These images show an increase in upward ambient light in the countryside of typically 25% during the seven-year period. Between 1993 and 2001 we have also seen increasingly widespread use of modern optical systems in road lighting, although poorly controlled luminaires continue to be employed. Over the same period there has been significant growth in other lighting, often of a less controlled nature, such as window lighting from shops, security lighting of commercial and other premises, sports facilities and churches.

Increasing awareness of light pollution issues is leading to more local authorities adopting light pollution policies.



These two images (normal exposure top, exaggerated contrast bottom) demonstrate the relative emissions into the night sky at the A10 roundabout, Puckeridge, Hertfordshire. To the left are G6^[1] 'flat glass or FCO' luminaires lighting the roundabout whilst the 'balls of light' to the right are low pressure sodium 'deep bowl, SCO' luminaires of no G class lighting the dual carriageway beyond.

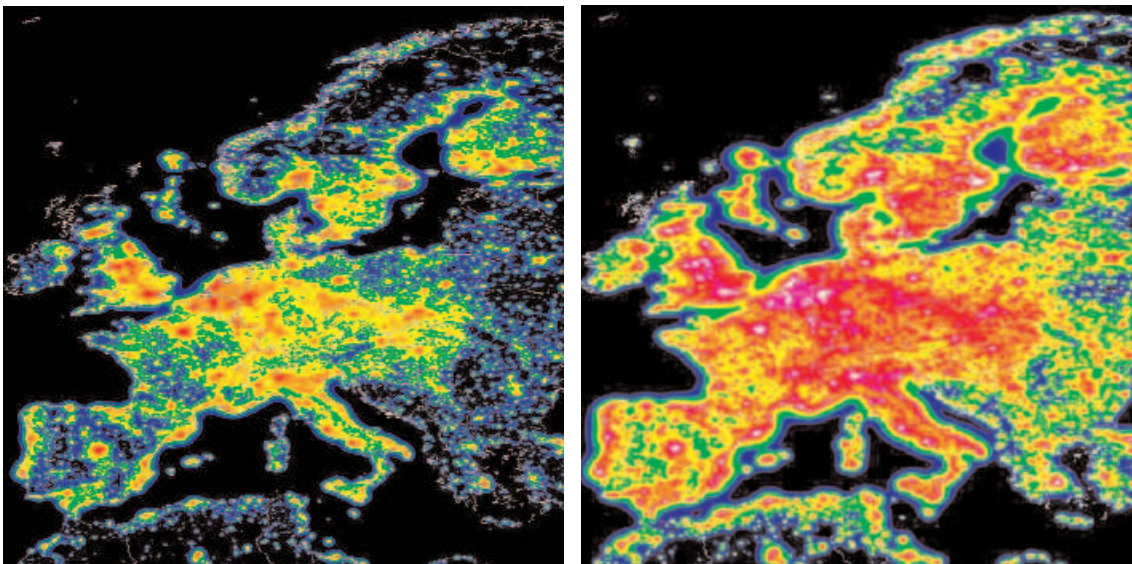


^[1] Under the current codes of practice for lighting in the British Isles, BS5489-1:2003 and BS EN13201-2:2003 the relative upward distribution of light from luminaires can be categorised by their 'G class' rating. This is found in Annex A on BS EN13201-2 and categorises luminaires into 6 classes. Classes 4, 5 and 6 equate to the older classification 'full cut-off', while 'semi cut -off' and 'cut-off' classifications are now replaced with G1 and 2 and G3 respectively.

In 2003, the Parliamentary Science and Technology Committee investigated and reported on light pollution and astronomy. The BAA Campaign for Dark Skies and the Institution of Lighting Engineers, like many other organisations, submitted evidence to the committee. The report to Parliament explained that light pollution was a growing problem affecting the majority of the population of the United Kingdom. (For example most of our population can no longer see the Milky Way from where they live). The report made a number of recommendations. The central one was to make exterior lighting falling outside the area intended to be lit to be defined as a statutory nuisance. It was also proposed that light pollution should be afforded the same status as other forms of pollution, and people who are troubled by it should have some legal redress. The Clean Neighbourhoods and Environment Act 2005 has gone some way to addressing this point, but as street lighting is exempt on grounds that light emitted is not from premises, and many other premises being exempt altogether, there is clearly still a long way to go.

If we do nothing, then skyglow is expected to dramatically increase over the next 20 years, as has been shown on the European prediction map of skyglow by P Cinzano et al. By 2025 the Milky Way will only be visible in a few locations across Europe and in Britain one would have to travel to North West Scotland in order to see any but the brightest stars

Although most lighting practitioners would prefer to use properly-directed lighting, a significant proportion of new lighting is still being installed with little input from qualified lighting practitioners. Examples of poor new lighting include low pressure sodium lamps installed as a perceived energy saving option, and modern well-designed products that are simply installed incorrectly.



Maps showing estimated growth of skyglow from 1995 compared with 2025 based on no changes in curbing skyglow as demonstrated by Cinzano, Falchi and Elvidge. These illustrations show the relative progressive growth of skyglow based on satellite imagery compiled in 1993 and again in 2001 and extrapolated forward to 2025. In creating these images based on satellite imagery an assumption has been made that there is a direct proportional correlation between light escaping the atmosphere to be recorded by the satellite and the ground-based observation phenomenon of skyglow. The computer modelling described later in this document confirms this and further refines our understanding of skyglow.

Skyglow: an executive summary

There is a lack of understanding of the subtleties of the mechanisms responsible for skyglow. To help understand the phenomenon, a computer modelling program was designed and used to demonstrate the mechanisms at work, and their relative contributions to skyglow. The model looks at the level of skyglow caused by specific types of luminaires, allowing different designs to be compared. The results could have significant implications on future lighting design for exterior lighting.

The concern is that increasing skyglow in the countryside prevents much of the population from seeing the wonder of the night sky. The computer model works for conditions of moderate to good visibility. It was originally designed to investigate skyglow in rural locations where the dominant light source is from nearby towns. It is not intended for use in town centres, where multiple types of light source, complex surface scattering and direct upward light obscure all but the brightest stars.

Sources of light pollution are numerous, but are increasingly derived from sports facilities and commercial, safety and security lighting. In general skyglow remains mostly orange, lasts all night long, and is dominated by road lighting. Skyglow in rural and semi rural areas caused by urban and suburban illumination can be controlled by using suitably designed or modified lighting.

The major features of skyglow for locations outside towns, on nights with good visibility and from light sources in towns can be briefly summarised as follows:

- Skyglow seen at a distance at any given view elevation angle (angle of observation into the sky measured from the horizontal) is the sum of the scattering from all source-illuminated air molecules and suspended particles along that line of sight. For the particles over the source, ground reflected light dominates, but its contribution to the total decreases with distance from the source as direct low angle light becomes more significant.
- For luminaires with significant direct radiance above the horizontal, the contribution from upward light forms a second peak in front of the individual sources that can far exceed that from ground reflection over the source. This is enhanced by the forward scattering properties of the atmosphere.
- At view distances of tens of miles, the limited effective height of the atmosphere and path geometry also enhances the contribution from shallow angle direct radiance. Overall this is at least 10 times the contribution from ground reflections.
- The reflected light component of skyglow is from roads, and also significantly from surrounding surfaces such as grass in suburban areas.
- The lower the cut-off angle, the less skyglow is caused; this is also true below the horizontal.
- The worst source of road lighting is the low pressure sodium (SOX) lamp equipped luminaire. Although the market for these luminaires is in decline, a significant quantity are still being installed each year. Shallow bowl high pressure sodium (SON) lamp equipped luminaires also contribute to skyglow at rural distances.

Skyglow photometry of night sky images in rural areas

For comparison purposes, a photometric study was made of skyglow images from rural locations. Several different image types were used including composite all-sky and fish eye lens images of the whole horizon.

AstroArt© software was then used on the images to obtain relative pixel brightness levels from the horizon to the zenith. Many stars were identified in these frames. For known stars, the brightness of the pixels with surrounding areas were taken and compared with adjacent areas to determine their true brightness within limits of saturation. Their evaluation was then used to obtain relative atmospheric extinction for the brightness and the calculated values were compared with the true stellar magnitudes^[2] (brightness). Conversion from point brightness to surface luminance and comparison with the corrected pixel values gave an indication of the lower limit of the skyglow in terms of magnitudes per square arc second, for a given elevation. The figures were approximate and prone to sensor non-linearity.

Skyglow in rural UK between towns is about magnitude 19 to 21 per square arc second at high elevations (equivalent to 8 to 1.5 millilux on the ground).

In a dark clear sky, one can see stars to magnitude 6 and there are several thousand stars per hemisphere. The total brightness from all starlight on the ground is less than 1 millilux; full moonlight is about 0.27 lux. A single bright star is about 1 microlux. The total contribution from the sky of stars is always less than the man-made skyglow.

Results were obtained from analysis of a fish-eye lens photograph of the Cotswolds and Avon region near Bath and Chippenham by Michael Tabb, and also a composite charged coupled device (CCD) image by James Weightman.

The stellar images suffered from saturation in the brightest parts, and saturation by the skyglow at its maximum, but typically the range from near the horizon over the towns to the zenith exceeds 40 to 1. The ratio of the darker parts on the horizon to the brightest is about 5 to 1. The curves steeply drop in the first few degrees away from the

^[2] The stellar magnitude (m) of a star, planet or other celestial body is a measure of its apparent brightness as seen by an observer on Earth. The brighter the object appears, the lower the numerical value of its magnitude. The scale upon which magnitude is now measured has its origin in the Hellenistic practice of dividing those stars visible to the naked eye into six magnitudes. The brightest stars were said to be of first magnitude ($m = 1$), while the faintest were of sixth magnitude ($m = 6$), the limit of human visual perception (without the aid of a telescope). Each grade of magnitude was considered to be twice the brightness of the following grade (i.e. a logarithmic scale). This somewhat crude method of indicating the brightness of stars was popularised by Ptolemy in his *Almagest*, and is generally believed to have originated with Hipparchus. This original system did not measure the magnitude of the Sun.

In 1856, Pogson formalised the system by defining a typical first magnitude star as one that is 100 times as bright as a typical sixth magnitude star; thus, a first magnitude star is about 2.512 times as bright as a second magnitude star. Pogson's scale was originally fixed by assigning Polaris a magnitude of 2. Astronomers later discovered that Polaris is slightly variable, so they first switched to Vega as the standard reference star, and then switched to using tabulated zero points for the measured fluxes. The magnitude depends on the wavelength band.

The modern system is no longer limited to 6 magnitudes or only to visible light. Very bright objects have negative magnitudes. For example, Sirius, the brightest star of the celestial sphere, has an apparent magnitude of -1.46 . The modern scale includes the moon and the sun; the full Moon has an apparent magnitude of -12.6 and the Sun has an apparent magnitude of -26.73 .

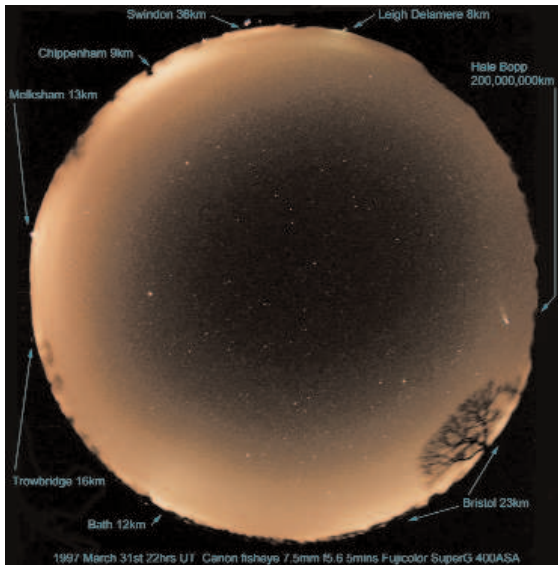
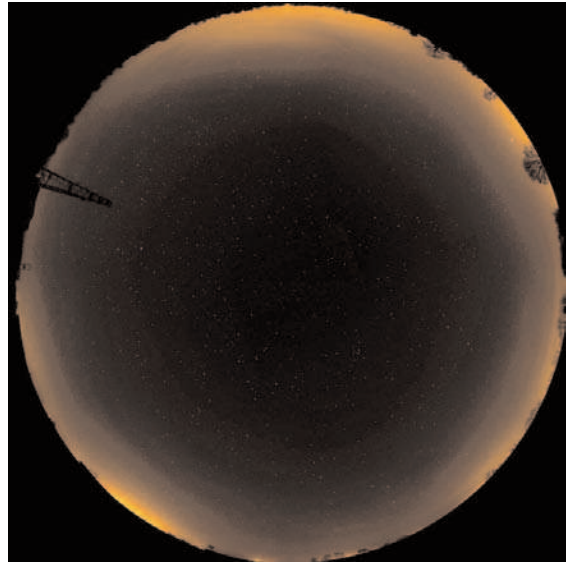


Image of skyglow in the Cotswolds, by Michael Tabb. A fish-eye lens image used for initial photometry of observed light pollution.

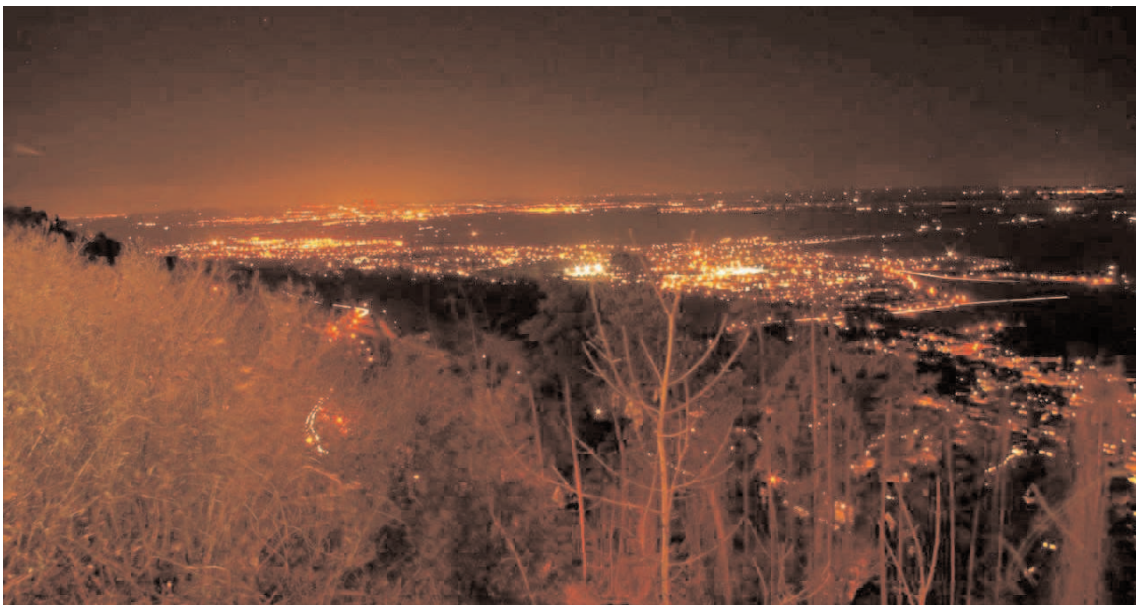


Skyglow elsewhere in the Cotswolds, by James Weightman. A composite CCD image used for initial photometry of observed light pollution.

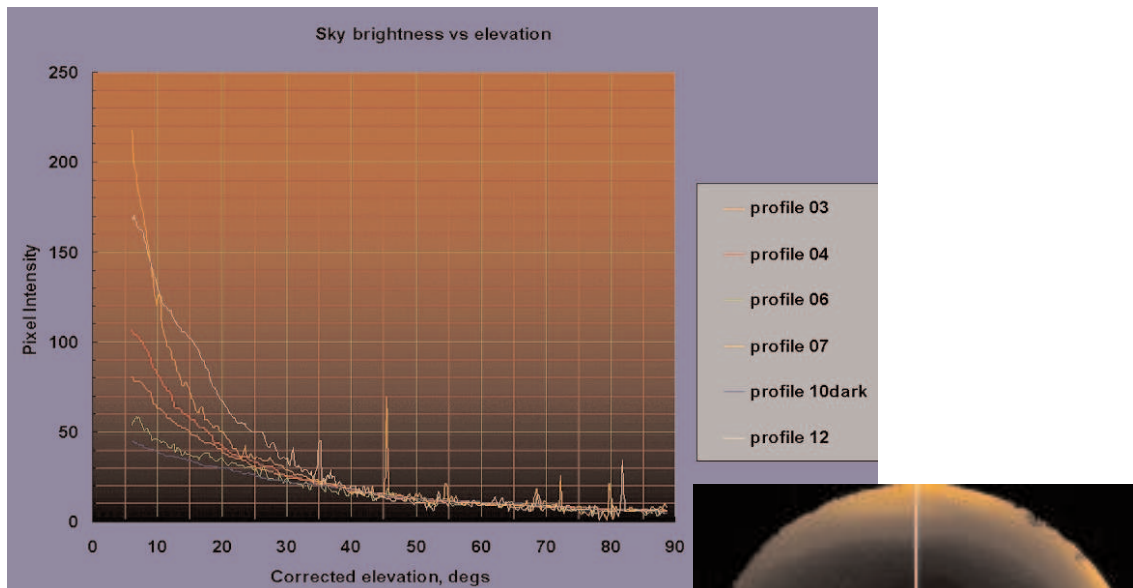
horizontal and then shallow off towards the zenith. But even at high elevations there is significant skyglow. This is much larger than may be apparent from the images, due to the compression in elevation versus azimuth (see the tree at bottom right in the Michael Tabb image).

Other images were analysed similarly.

Since then a further study at a fixed semi-urban location (Malvern) recording precise photometry of the near zenith sky was made over a period of three months in all weathers. The sky brightness varied by 30 to 1 according to air clarity and cloud cover. In low cloud, the skyglow achieved 100 millilux.



Worcester from the Malvern Hills. This image shows the extent of individual luminaires emitting towards the camera, seen here at many degrees elevation above the horizontal. (Dr. Christopher Baddiley)



Pixel intensity extracted from photographic image from horizon to zenith.

Mathematical modelling of skyglow

There are four mechanisms at work that cause skyglow, and each needs to be considered in the computer modelling:

- 1 directly radiated light above the horizontal;
- 2 reflected light (specular and scattered), from the road, ground and other surfaces;
- 3 light scattered by air molecules; and
- 4 light scattered by aerosols (particles of dust and water droplets, ranging from slightly smaller to much larger than the wavelengths of light).

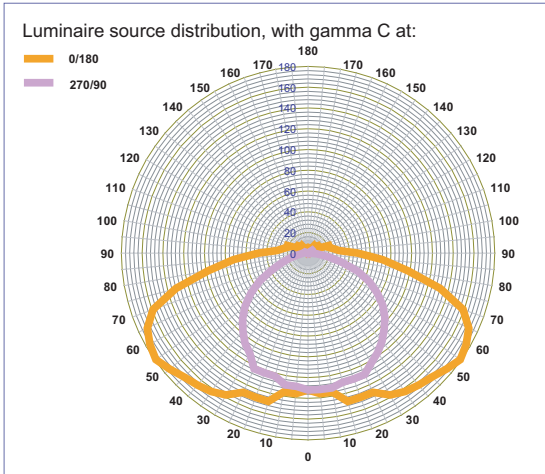
The luminaires

Manufacturers' luminaire photometric data was used in the computer model. For this study, three types were considered:

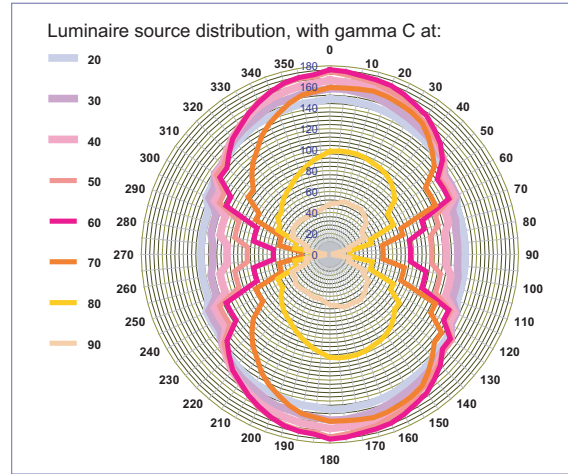
- 1 a low pressure sodium lamp (SOX) equipped side-entry luminaire;
- 2 a high pressure sodium lamp (SON) equipped, G3, cut-off or shallow bowl luminaire;
- 3 a high pressure sodium lamp (SON) equipped, G6, full cut-off luminaire with flat glass glazing.

To investigate the effect of changing the spectrum, these last two were additionally modelled as white light versions equipped with ceramic metal halide lamps (CDM).

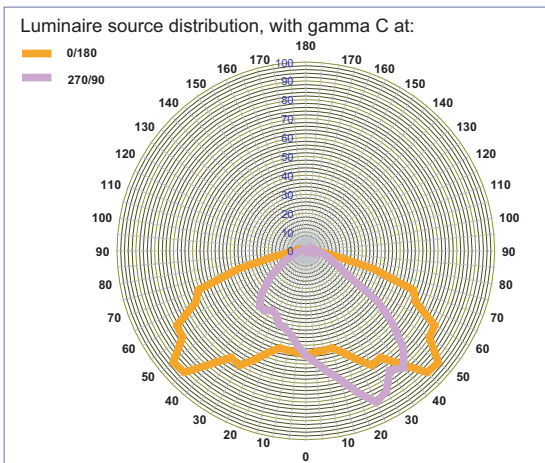
Polar diagrams were made for each of these three basic cases for C angles along the road and then across the road. Plots were also made in gamma angles up to the vertical.



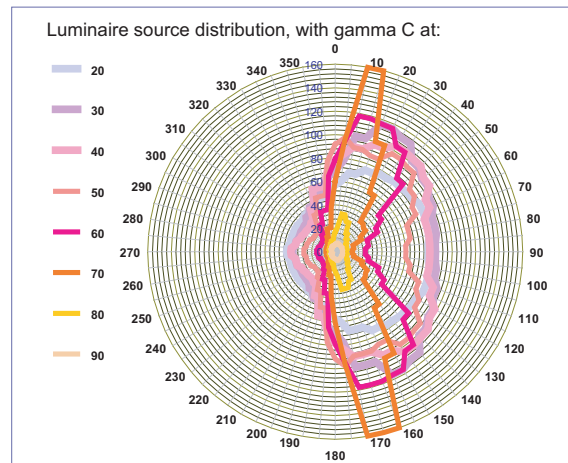
Polar diagram 1: Elevation polar diagram of a SOX luminaire at C angle 0–180 and 90–270.



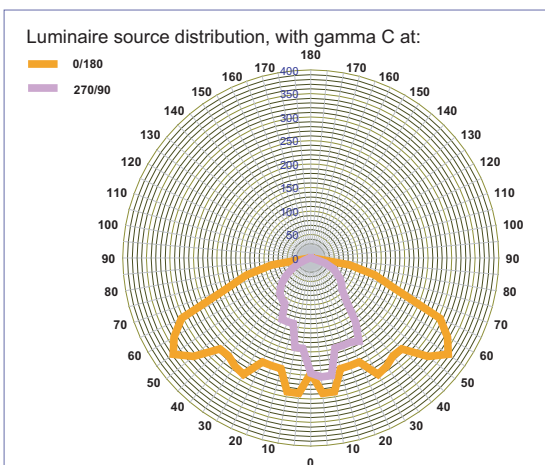
Polar diagram 2: Horizontal polar diagram of SOX luminaire for C angles 0–360, stepped every 10° at gamma angles of 90 to 180°



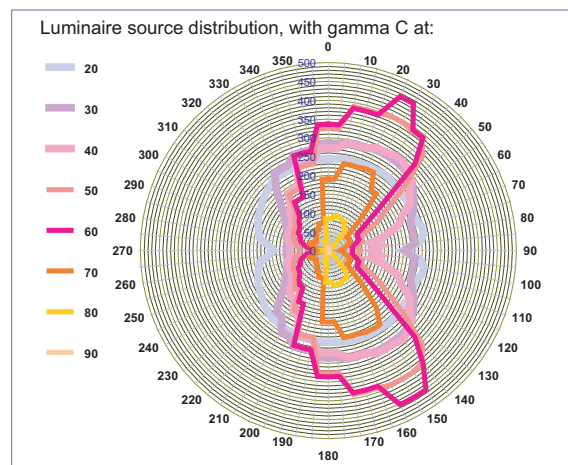
Polar diagram 3: Elevation polar diagram of a cut-off (G3, shallow bowl) luminaire at C angle 0–180 and 90–270.



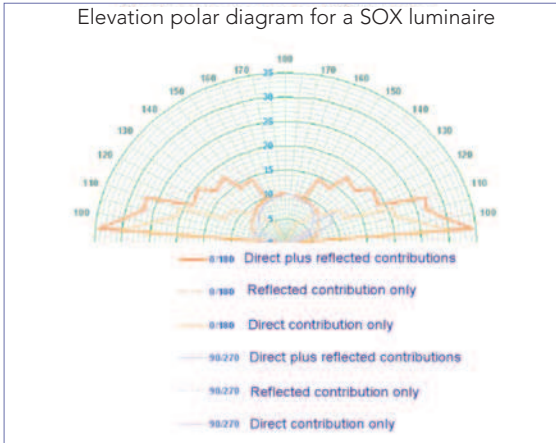
Polar diagram 4: Horizontal polar diagram of a cut-off (G3 shallow bowl) luminaire for C angles 0–360, stepped every 10° at gamma angles of 90 to 180°



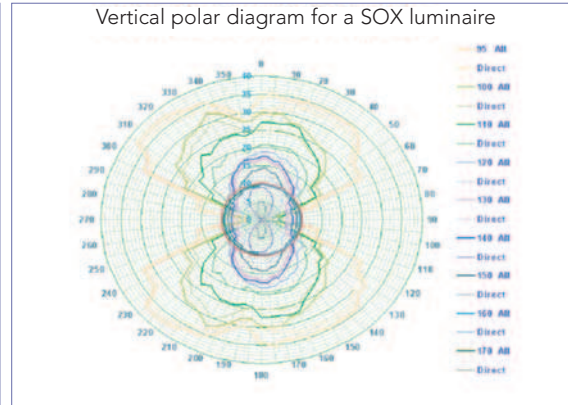
Polar diagram 5: Elevation polar diagram of a full cut-off (G6) SON luminaire for direct and reflected (specular and scatter) and combination at C angle 0–180 and 90–270 for gamma 90 to 180.



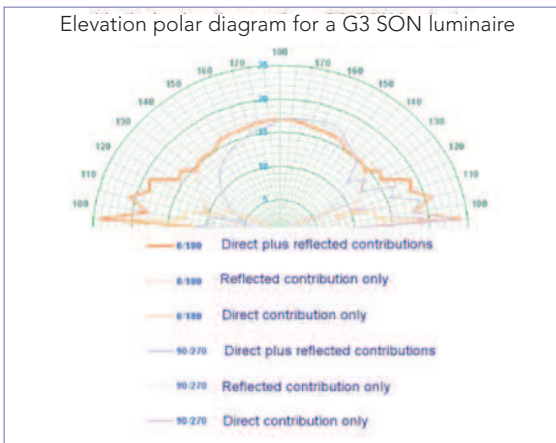
Polar diagram 6: Horizontal polar diagram of a full cut-off (G6) SON luminaire for C angles 0–360, stepped every 10° at gamma angles of 90 to 180°.



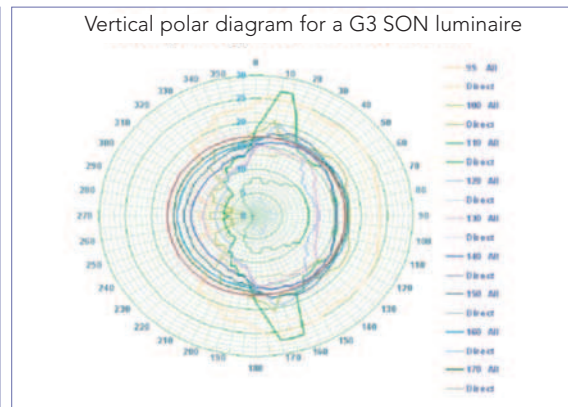
Polar diagram 7: Elevation polar diagram of a SOX luminaire for direct and reflected (specular and scatter) and combination at C angle 0–180 and 90–270 for gamma angles of 90 to 180°.



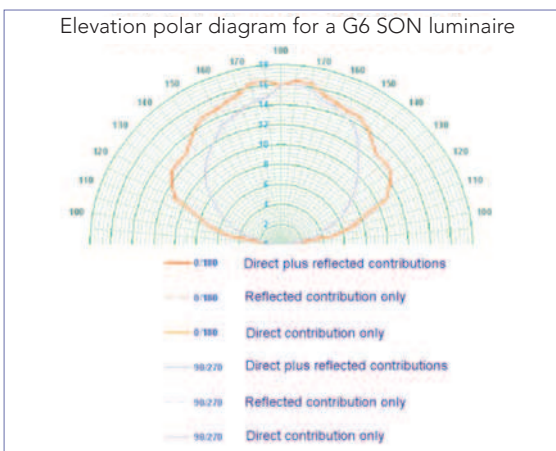
Polar diagram 8: Horizontal polar diagram of a cut-off SOX luminaire for direct and combined reflected (specular and scatter) for C angles 0–360, stepped every 10° at gamma angles of 90 to 180°.



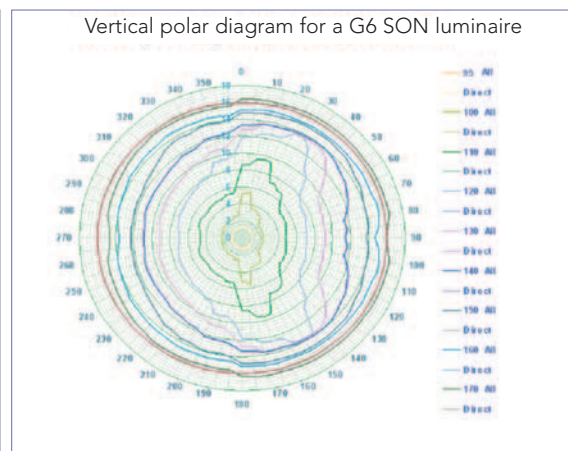
Polar diagram 9: Elevation polar diagram of a cut-off (G3 shallow bowl) luminaire for direct and reflected (specular and scatter) and combination at C angle 0–180 and 90–270 for gamma 90 to 180.



Polar diagram 10: Horizontal polar diagram of a cut-off (G3 shallow bowl) luminaire for direct and combined reflected (specular and scatter) for C angles 0–360, stepped every 10° at gamma angles of 90 to 180°.



Polar diagram 11: Elevation polar diagram of a full cut-off (G6) SON luminaire for direct and reflected (specular and scatter) and combination at C angle 0–180 and 90–270 for gamma 90 to 180.



Polar diagram 12: Horizontal polar diagram of a full cut-off (G6) SON luminaire for direct and combined reflected (specular and scatter) for C angles 0–360, stepped every 10° at gamma angles of 90 to 180°.

Reflectivity

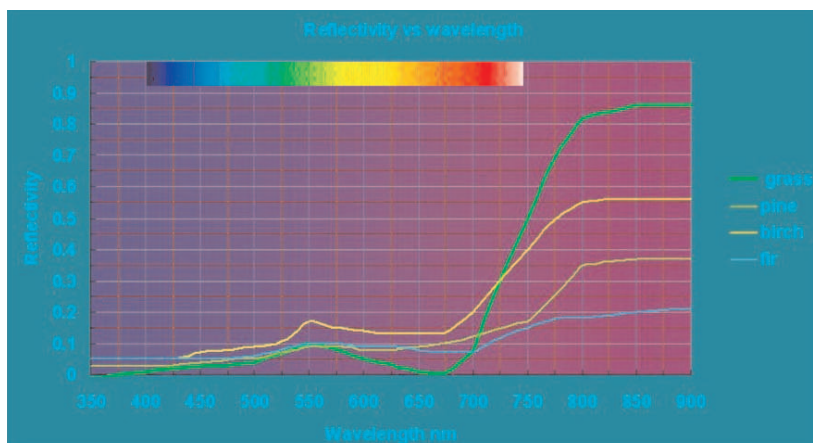
The reflectivity of all surfaces increases away from normal incidence. This is determined by Fresnel's equations based on refractive index; the increase is also dependent on normal incidence reflectivity. For smooth surfaces, there is some angle where horizontal polarised light is not reflected, causing a significant drop in the overall reflectivity. For rough surfaces, the more appropriate form is the Lambertian function (usually referred to emissivity) where apparent reflectivity varies as 1 minus the cosine of the incidence to normal angle. Surfaces increase in reflectivity to unity values at grazing incidence. Real surfaces are rough and partially scatter light in all directions, varying with the apparent projection of the surface area, i.e. as the cosine to normal incidence. The specular reflection distribution is dependent on the facet angle distribution through a convolution, which was not modelled due to its complexity and its relative lack of effect on skyglow. A surface roughness factor was used to set the ratio of specular to pure scatter reflections as an approximation to true surface bidirectional reflectance distribution functions (BRDF).

It is common experience in observing car headlights on roads at night that one sees an image and ripple glitter path from the lights on the road peaking at the specular reflection angle. Street lights behave similarly, which is particularly clear when the surface is wet.

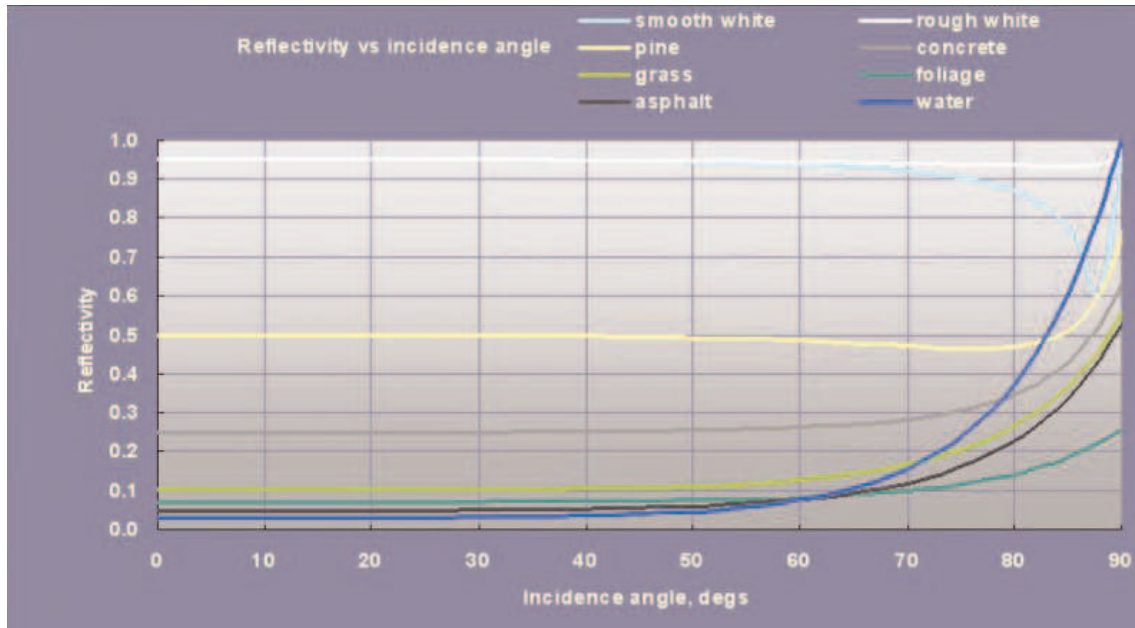
Much of the light from luminaires on the ground falls outside of the road area. So the model computes the reflections from two surfaces, asphalt for the road and grass for the surroundings, and a third for vertical surfaces if present.

The reflectivity at normal incidence for grass is only 0.1 at its peak wavelength, and in common with all vegetation, is low at the photosynthesis absorbing wavelength of about 640 nm, before rising sharply in the near infrared. The reflectivity in the yellow and blue are quite similar. Grass reflectivity increases by about 2 times at 70° from the vertical. The spectrum of grass and its variation with incidence angle is modelled within the program.

Asphalt reflectance varies considerably as indicated in the published R tables in BS EN 13201 but is typically around 0.05 depending on its cleanliness, (CIE British asphalt at 0.07 seems to be less common than many would suppose) but in common with most smooth or semi-smooth surfaces increases towards grazing incidence. This corresponds



Reflectivity of grass by wavelength.



Theoretical reflectivity of materials by angle of incidence. Note the polarisation 'dip' on the more specular materials and how towards grazing angles all materials tend towards specularity

to light emitted just below the horizontal which is by default highly reflected into the sky. Concrete and brick reflectivity at normal angles of incidence is nearer 0.25.

The scatter reflection and its luminance in any given direction requires a summation over all angles and surfaces before its projection can be calculated. These values are stored for repeated access. The component is added to the specular part for the view angle.

The upward light output ratios (ULORs), ground reflections, and total upward ratios are shown below.

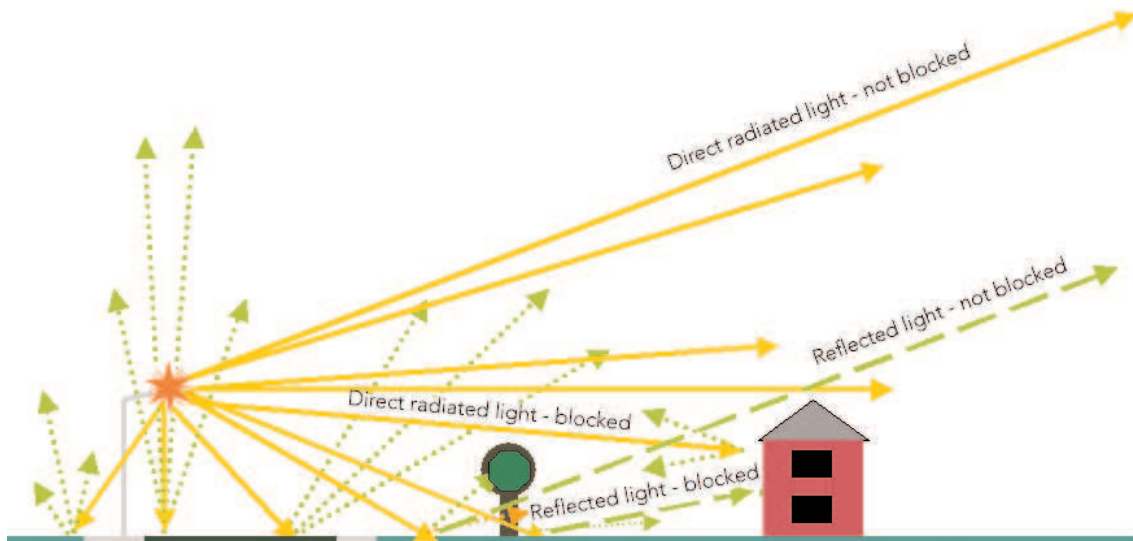
Luminaire	ULOR	Ratios to total	
		Total reflected	Direct and reflected
SOX (5° tilt)	7.9%	4.6%	12.5%
SON cut-off (G3)	3.2%	4.8%	8.0%
SON full cut-off (G6)	0.0%	5.7%	5.7%

Luminaire upward light and reflection distributions

Low angle reflections are invariably blocked and partially reflected upwards by obstructions on the ground such as trees, buildings and topography. This is modelled when vertical surfaces are defined, but has not been included in this study.

Light distribution polar diagrams were generated for both the upward radiated and reflected components. An integration routine was written to give totals of component parts over a sphere or upper hemisphere or parts of a hemisphere for direct radiated and also reflected light. These values were compared for the three types of luminaires considered.

Asphalt roads are represented in the model and pole height, overhang and road width are defined (for example pole height 8 m, set back 1m and overhang 1m for a 10m wide road).



Reflected and direct components of light emissions affecting skyglow.

Atmospheric scattering

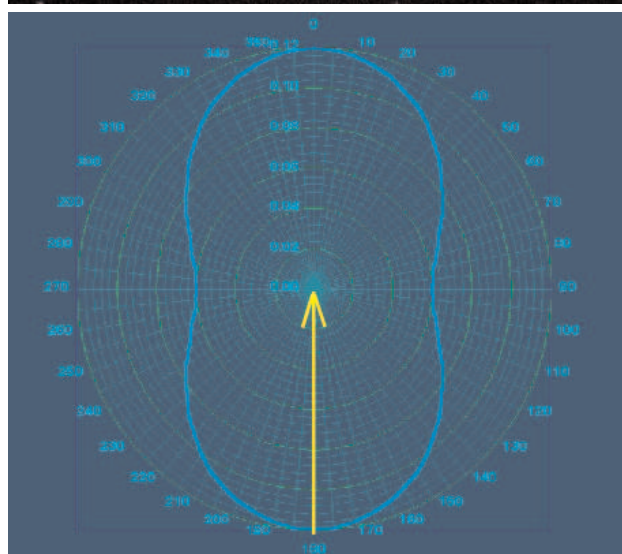
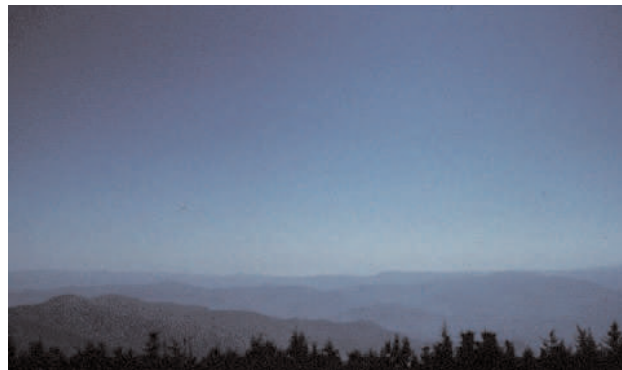
A function was designed in the model to represent the variation of density of dust particles and air molecules with altitude in the atmosphere. At 10 km altitude, the air density is reduced to nearly half its ground value. This reduces the amount of scattering with altitude and differs for each scatter type.

When considering air scattering, it is important to note that there are two main scattering types that have very different scattering properties.

Scattering by air molecules

Air molecules are far smaller than the wavelength of light. They scatter light forwards and backwards equally, and scatter light sideways at half the forward intensity. They are very much more effective at scattering shorter (bluer) wavelengths. This is known as Rayleigh scattering, and is the reason why the sky appears blue.

Rayleigh scattering. In this diagram the light path is indicated by the yellow arrow. Note that significant quantities of light are scattered forward and backwards but there is only around half the scatter to the sides.



Scattering by air borne particles (aerosols)

Aerosols are suspended water droplets and dust particles with sizes ranging from less than to much greater than the wavelength of light. These scatter light sharply forwards, very little sideways, and only very slightly backwards, and are not affected by wavelength. This is known as Mie scattering, and is why clouds appear white.

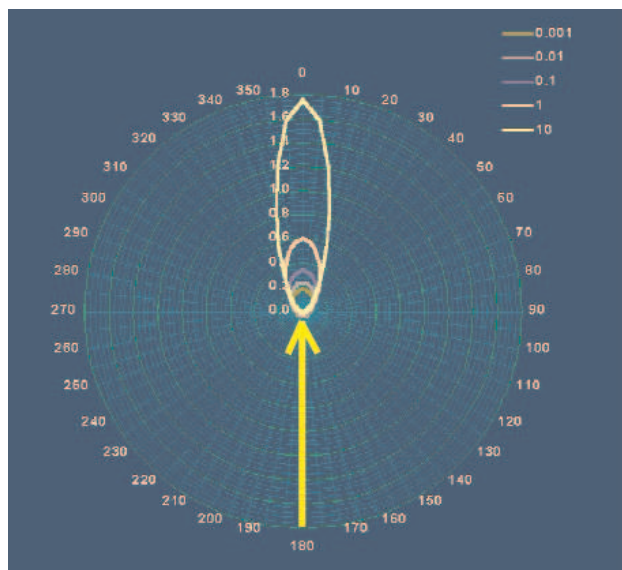
The computer model calculates single scattering, i.e. scattering from centres along the view path directly illuminated from the source or ground. Multiple aerosol scattering can produce orthogonal and even retro-reflection, as is sometimes seen in mist or clouds. The model approximates this. But these are features of poor atmospheric conditions. We are only concerned with skyglow in good atmospheric conditions, as in poor conditions there is no view of a starry sky anyway.

Contributions from multiple scattering and multiple sources can be approximated in the program, but to do this thoroughly would be too demanding on processing time.

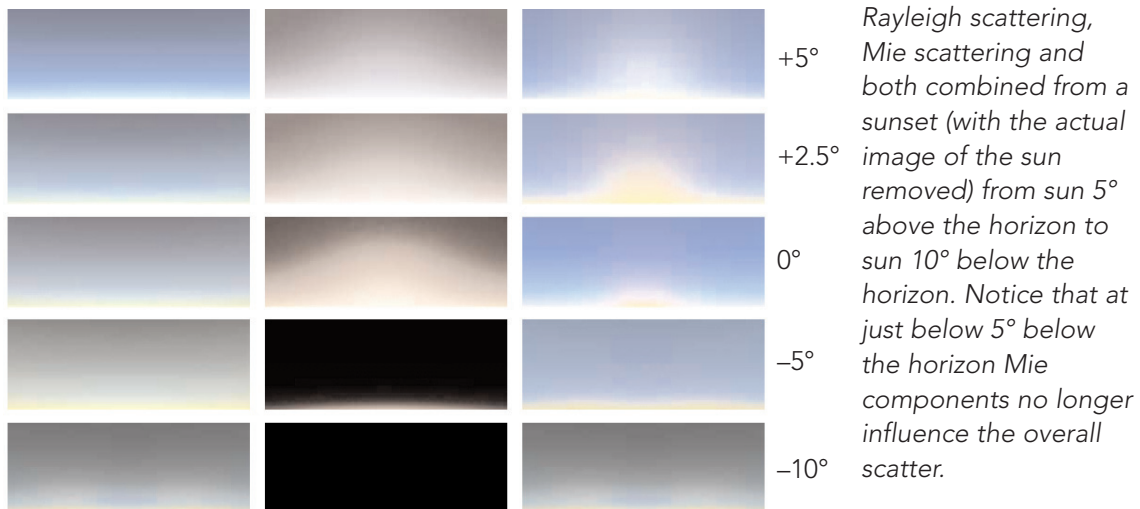
Geometry

The atmospheric program starts by specifying a given view angle elevation path out to a given distance from the source. A set of points along that path are specified and the distances and scatter angles to the source calculated. In determining the extinction along a given path through the atmosphere, each height density increment must be summed and scaled along the view path and the source path. The local scatter angle at each point along the view path is also determined for use by the scatter types and angle probability functions. This scatter into view per path increment is plotted.

Viewing distance and elevation is selected or made a controlling variable according to what is to be plotted. The illuminated intensity at a particular particle location varies as the inverse square of the distance from the source. The sky is treated as a surface of luminance per solid angle cone of view. The sky luminance after scattering is then independent of scattering location to observer distance, apart from extinction. That is not so



Mie scattering. In this diagram the light path is indicated by the yellow arrow. The larger the scatter particle, the more forwards the scatter beam.



for the illuminated scatter particle, where the inverse square law from the source and extinction applies.

Scattering increment

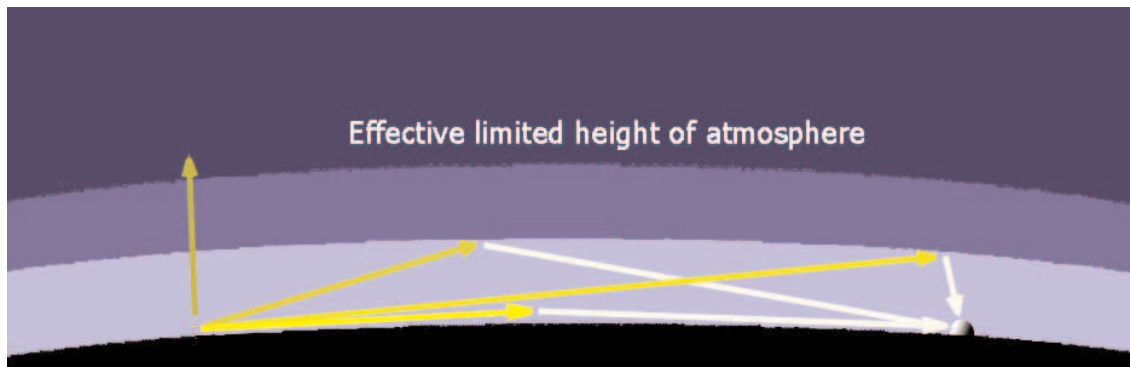
If we consider a small increment of path, then the fraction of light scattered out of view by that increment is proportional to the scatter probability^[3], the density of scattering particles and the length of the increment. The next adjacent increment receives the output from the previous one, and so the output becomes a fraction of a fraction of a fraction and so on. If the scatter angles and densities were constant (which they are not) then this would sum along a path to a negative exponential, the normal extinction curve.

The amount of light that is scattered into the path must be proportional to the amount of light that is scattered out of it.

A given view path is divided into sample view path increments increasing in size, from viewer to space. Both the path volume increment along the cone of view varies in projection solid angle seen from the source. The scatter increment length is geometrically related to this and the local scatter angle. All these are calculated in three dimensions, for each scatter increment along the view path in any selected direction from the source. These are then multiplied by the local scatter density as a function of altitude, and the scatter probability for each scatter type. This is multiplied by the source illuminance after extinction as previously described, taken from the source direct and reflected luminance by all possible surface reflection paths to the source, where the view angle is that seen by the scatter point location. After applying the path extinction, the values for each path increment are added over the view path to space to give the apparent skyglow brightness in that line of sight view direction.

The program does a full path summation for each sky viewing elevation, taking into account all the variables that are described above.

^[3] For the purpose of modelling pure scatter in angular effect, this may be summarised as that fraction of the light incident on the scattering particle that is scattered into unit solid angle (1 steradian), at any particular given angle measured from the original incident direction, compared with that over all directions (4π steradians).



The relative importance of ground reflected to direct light, and aerosol to molecular scattering

After sunset, the aerosol (Mie) scattering stops when the sun is 5° below the horizon while molecular or Rayleigh scattering continues well beyond that. (See <http://webexhibits.org/causesofcolor/14B.html> for a detailed explanation of this and related phenomena).

Rayleigh scattering is therefore dominant only at high view elevations. The aerosol scattering is highly concentrated in the direction of the source, which at rural distances is close to the horizon. The largest scattering contribution to the line of site occurs in front and above the source, and is Mie scattering. At such low source elevation angles, ground obstructions stop the reflected components from contributing much.

Directly over the source, Mie aerosol scattering through near right angles towards the rural observer is insignificant. Here molecular scattering dominates, but at very much lower levels.

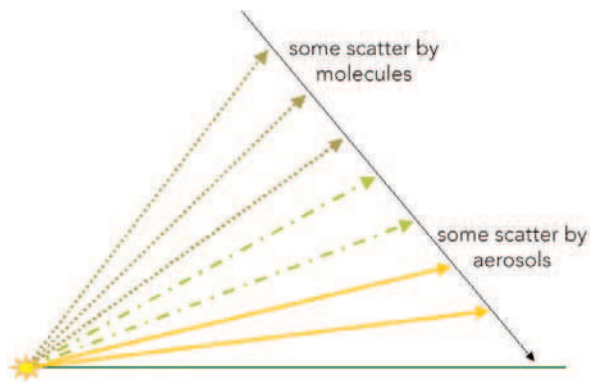
Therefore any direct light travelling just above the horizontal is a major contributor to skyglow. Ground reflected light is typically a factor of 10 lower depending on ground reflectivity.

Light going straight up from towns has less effect on skyglow on clear nights in rural locations, than that travelling sideways. This is important as it can be easily prevented by using modern luminaires with well-controlled upward light emissions.

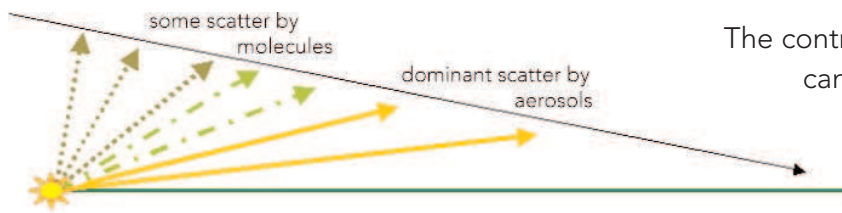
Overcast or misty skies are a different matter, but that is not when people are looking at stars and so is not within the remit of this study.

Output plots from the program

For the comparison skyglow modelling, all the luminaires were rescaled to give the same overall luminous output at a selected gamma angle along the road. A SOX luminaire, a cut-off (or G3) luminaire and a full cut-off (or G6) luminaire were each evaluated, as were white light versions of the last two.

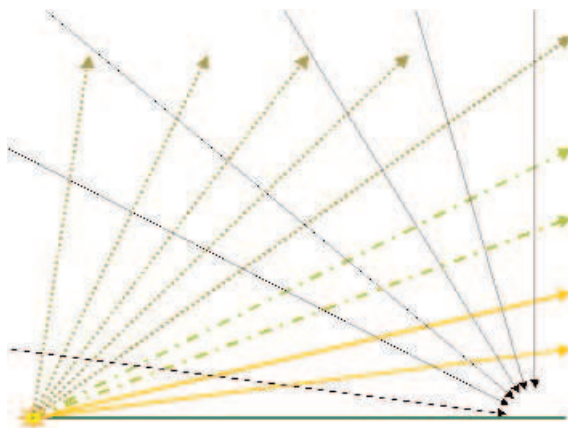


An observer at a given distance from the source and at a given view elevation to the sky, receives light that is scattered at all points along his view path to space. The program plots the incremental gradients, i.e. the contribution to light scatter in each section of a given elevation path. This is plotted for the three luminaire types – see figure captions on the following pages for a detailed description.



The contributions from aerosols can be varied through atmospheric visibility (23 km is good, below 5km is bad).

The aerosol contribution





is also shown removed in the dotted curves in the plots.

The program also plots the sum of the scatter along that path for stepped elevations from the horizon to the zenith and on to the far horizon, also for the three luminaire types.

Finally, total skyglow is plotted as a function of distance from the light source for a given fixed 45° elevation.

Key to diagrams

-  Mostly reflected light
-  Mixed light
-  Mostly direct light

The components of scattering into the angle of view can be calculated for any viewing angle at any range from the source.

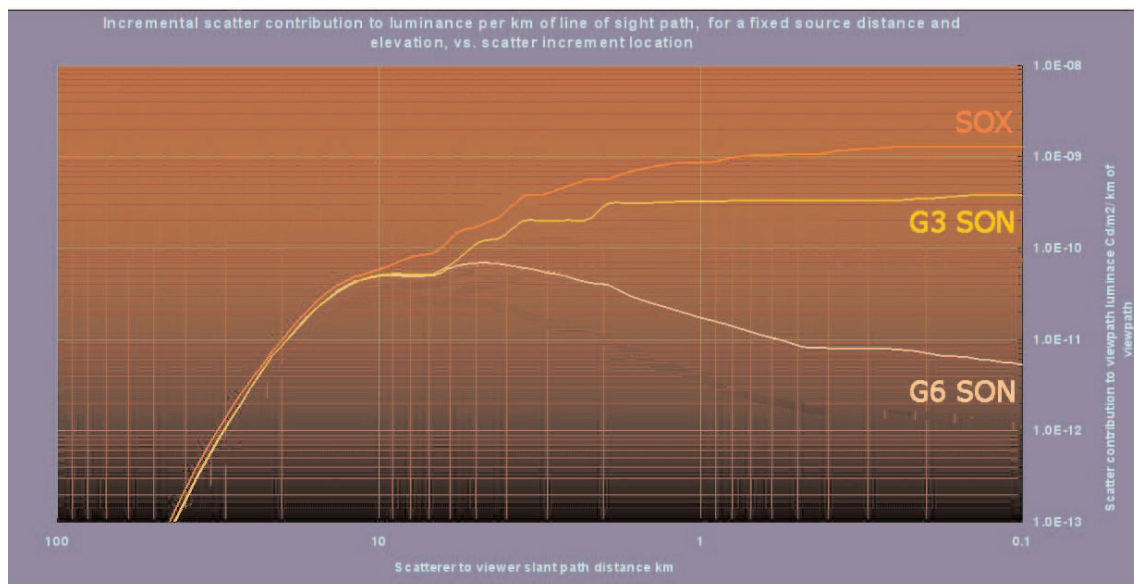
These results were also compared with the empirical Walker's law, which states that the skyglow from isolated towns should vary inversely as a 2.5 power of the distance. The gradient for cut-off luminaires when plotted on a log intensity versus log ground distance plot, does indeed approach -2.5 but at many tens of kilometres from the source.

Accuracy of modelling

By default the accuracy of the scattering modelling is compromised by the computational demands of the calculations necessary. Therefore single scattering has been modelled rather than multiple scattering. The best multiple scattering calculations available currently have been undertaken by Martin Aube of Quebec University using a super computer. The results achieved on this super computer correlate reasonably well with the simplified modelling in this adopted skyglow model.

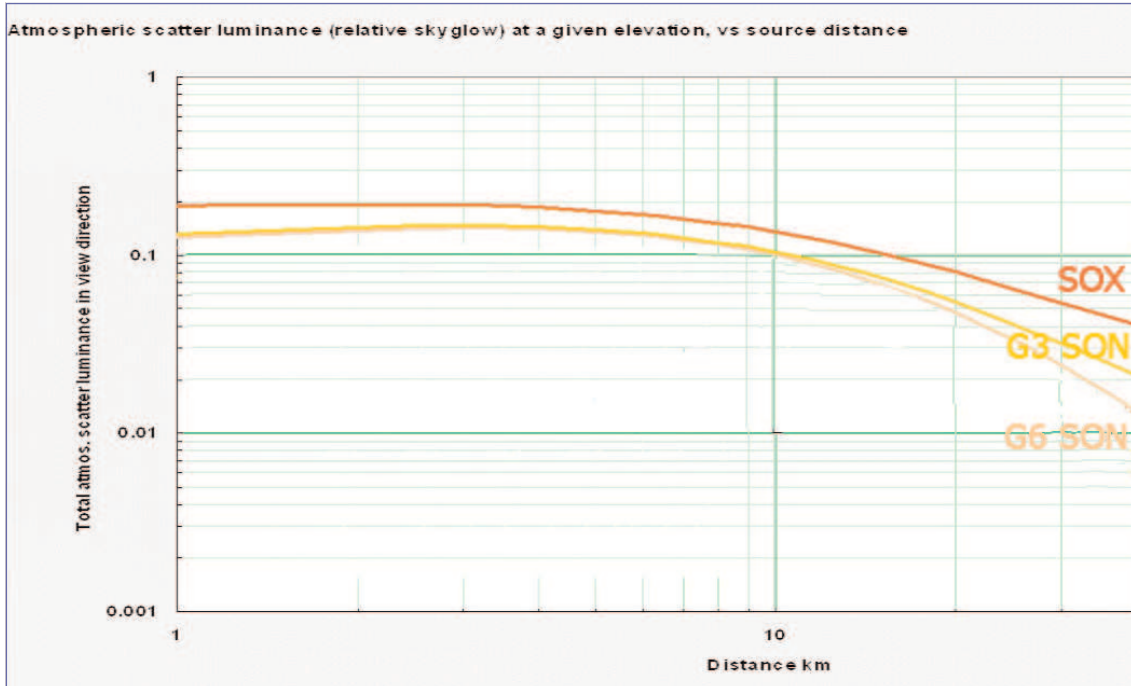
Rural skyglow dependence on luminaire types

The results show a strong dependence on the cut-off angle of the luminaire used. Low G class luminaires can emit a significant proportion of their radiation above the horizontal. Combined with the reflected components, they exceed in their contribution to skyglow by 50% or more compared to modern cut-off (G3) and full cut-off (G6) luminaires and by up to 5 times in view directions away from the source. Some shallow bowl (G3) luminaires have a slightly higher elevation distribution than full cut-off (G6) designs, causing more reflection at low angles, and also some side emissions. This may cause them to be more visually intrusive. They add more to skyglow compared with full cut off designs when seen at rural distances, although this does vary from design to design. They allow further column spacing so reducing the amount of upward light per road length, but the column spacing advantage needs to be considered against the increase in skyglow per unit.

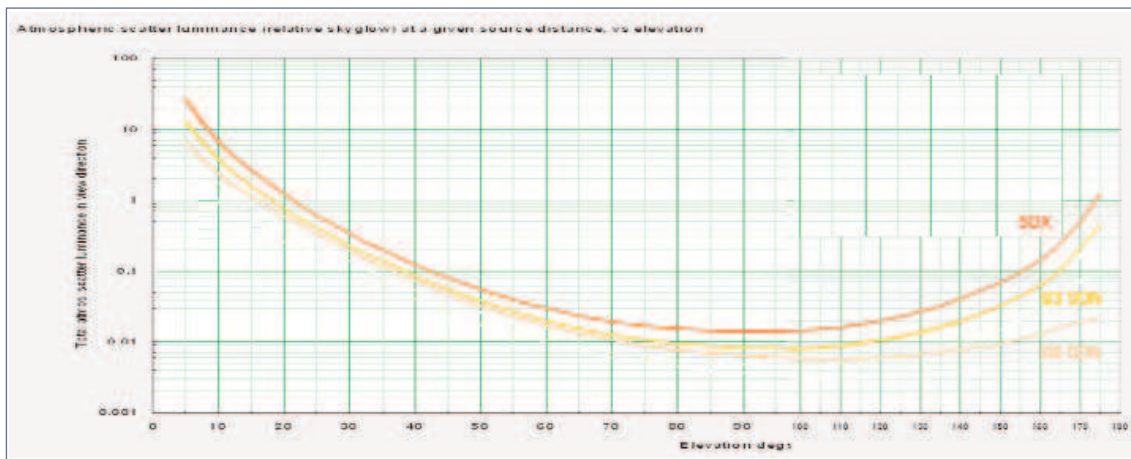


This diagram with a logarithmic horizontal scale shows the scattered light input per km path length, into the line of sight along a viewing path at 45° elevation, measured from the viewer, for each increment along the path. The source is at 20 km distance from the viewer. The viewer is at the right, and the source is far left of centre. On the left we see the back scatter from the atmosphere for scatter points beyond the source. At 28 km along the inclined viewing path, the scatter point is directly over the source and the scattering is near orthogonal and mostly from air molecules. This is the first peak on the left, for all three sources. The illumination of the scatter point is then ground reflection.

The greater peak at about 8 km along the line of sight from the viewer for the SOX luminaire (deep orange) is the effect of its direct radiance to the sky, causing excessive scattering in the lower atmosphere, due to its badly controlled output above the horizontal, scattered particularly by aerosols. Note in 'ideal' air with no aerosols (thin dotted curves), the SOX case has much less of a peak. The full cut-off luminaire (light orange) with no direct radiance, shows no forward scatter peak at all. The shallow bowl cut-off design curve lies above the full cut-off curve most noticeably at the nearer distances to the viewer. For all the luminaires, the luminance at a fixed gamma angle along the road was scaled to the same lamp flux. Dotted curves represent skyglow in ideal air with no aerosols.



This diagram, with logarithmic horizontal and vertical scales, shows the relative total skyglow luminance at a 45° elevation view path, as a function of distance of source to observer. The source is on the left. The observer moves from there to the right. Notice that SOX (deep orange) creates significantly more skyglow than the cut-off case (pale orange) at all ranges, especially at large distances beyond 20 km. It is visible after cut-off /shallow bowl (yellow) and full cut-off (light orange) SON are no longer contributing significant skyglow. The excess at large distances from the shallow bowl cut-off luminaire (yellow) can be seen.



This diagram on a logarithmic vertical scale, shows the relative skyglow luminance for all elevations, 0 to 180° over the sky, from horizon to horizon, into the angle of view, by SOX (deep orange) and cut-off / shallow bowl (yellow) and full cut-off (light orange) SON lighting. The viewer is 20 km from the source. Note that although at low viewing angles all have major impact, at any other angle it is again the SOX luminaires that are contributing by far the most to the skyglow at all elevations. The least is full cut-off SON. The differences are most apparent in the direction away from the source. Further work has shown that the effect of obstruction and upward reflections off buildings about the road is to reduce the skyglow a little, and at the same time significantly increase the lower parts of the curve. At closer distances, the curves become much less steep, as skyglow spreads through reflections to all elevations.

Luminaire type	Upward light ratio (fraction of total above horizontal)	Ground reflection	Upward fraction including ground reflection	Relative skyglow at 45° elevation to near zenith, 20 km distance (FCO=100%) for same luminance at gamma=45	Relative skyglow at 135° elevation, (FCO=100%) for same luminance at gamma=45
SOX (5° tilt)	7.9%	4.6%	12.5%	170%	450%
SON cut-off (G3)	3.2%	4.8%	8%	150%	230%
SON full cut-off (G6)	0%	5.7%	5.7%	100%	100%

The table summarises the results with that of the last plot. The relative flux differences between the SOX and SON lamps were equalised (set to the SON values) to yield a relative skyglow comparison.

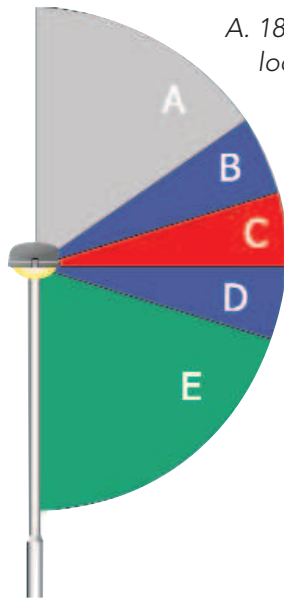
At a distance of 20 km, the SOX luminaire gave nearly 70% more skyglow than the FCO (G6) luminaire above 45° elevation and 350% more skyglow than the FCO facing away from the source; with the modern curved glass cut-off or G3 luminaire the results were in between these. In practice, the differences will vary with exact project design, and ground surface roughness. Identical luminaires differing only in flat glass (G6) to shallow bowl (G3), showed an increase in skyglow of 10 to 25% in an observer direction away from the source for the shallow bowled G3 luminaire.

The effect of the move from high pressure sodium towards white light sources was also investigated. Grass and other vegetation has a spectral peak in the green wavelengths. That together with the strong molecular wavelength dependent Rayleigh scattering demonstrates an increase of 75% in skyglow moving from 590 nm (sodium) to 550 nm peak wavelength light. It does not rise any more at shorter wavelengths due to a reduction in reflectivity. Operating white light sources at lower illumination levels to optimise their performance for scotopic vision towards the blue also applies to the visual perception of the scattering and so that alone gives little net benefit.

Summary

Skyglow in the countryside is dominated by stray light from towns, even 20 km or more away. This is still derived mostly from street lighting, although other lighting is on the increase – golf driving ranges and car parks being just two examples. Direct light emitted from G5 or lower class luminaires just above the horizontal travels through long path lengths in the lower atmosphere, and it is this that is mostly responsible for skyglow seen from rural areas. Curbing these low angle emissions must therefore form the focus of our efforts to minimise skyglow.

Diagram to show relative impact of a luminaire's output with regards to contribution to skyglow.



- A. 180–100° Critical area for skyglow experience from within urban and local areas but minimal impact to remoter (rural) viewing areas.
- B. 100–95° Significant contributor to skyglow, especially in rural areas where it is most aerosol dependent. Less likely to be obstructed.
- C. 95–90° Critical zone for skyglow seen at tens of km (in rural areas) where it is strongly dependent on aerosol scattering.
- D. 90–70° Significant contributor to skyglow seen at a distance through reflection but reflected light more likely to be obstructed by buildings, trees and topography.
- E.. 70–0° Ideal light distribution.

These low angle beams of light are preferentially scattered by aerosols (dirt, moisture and particles) in a forwards direction, while air molecule scattering dominates at high elevations. The widespread use of G3 luminaires could reduce much of the urban skyglow problem, and use of G6 luminaires could reduce the rural skyglow problem. G6 luminaires have a positive impact over large distances particularly beyond 20 km, and should continue to be encouraged, especially in rural (or open to rural view) projects.

The change from high pressure sodium to white light enhances scattering significantly where the higher reflectivity from grass and leaves and the strong blue bias of Rayleigh scattering from molecules is dominant.

Conclusions

The 2003 CPRE report 'Night Blight' has underlined the fact that light pollution has grown from 1993 to 2000 to such an extent that 'darkest England' has shrunk from 15% to 11% of our country, and over a quarter of the country had increased brightness through skyglow by one or more bands (as defined in that document). In short, skyglow in particular is on the increase and as a nation we must tackle it effectively to safeguard the night sky for future generations.

This document helps demonstrate the mechanics of skyglow and shows that minimising light emitted from luminaires at or near the horizontal is of paramount importance. However, this is merely one aspect of light pollution and we need to consider all aspects. The most fundamental question we need to ask in any given area is 'Do we need the light or not?' This may be a simple question for new projects, but what about old projects? Do they continue to require lighting? Are the levels still relevant or have the project parameters changed (for example de-trunking of a highway)? Where we need light we need to consider what lighting levels we actually require for the specific visual task. We then need to consider whether or not we are actually achieving our target objectives. Are we exceeding requirements? Can we use variable lighting? Brightening,



Comet Ikeya-Zhang over trees, from Suckley, Worcestershire. An example of what can be seen when skyglow is minimal. (Dr. Christopher Baddiley)

reducing and switching lighting gives us a very powerful tool with which to minimise future light pollution. Finally when we have completed our projects we must evaluate the results. Have we got it right?

If we undertake all of these measures we can work towards a future night time environment that is safe and stimulating, but also one where the sky at night has been returned to its original splendour through an understanding of the mechanisms of skyglow.

Bibliography

- British standards on road lighting BS5489:1 2003 and BS EN13201-2:2003
- "Guidance Notes for the Reduction of Light Pollution", Institution of Lighting Engineers.
- "Model for Artificial Night-Sky Illumination," R.H. Garstang, Pub. Astron. Soc. Pacific 98, 364 (1986).
- "Modelling Man made Night-Sky Illumination," R.H. Garstang, in Identification, Optimization and Protection of Optical Telescope Sites (eds. R.L. Millis, O.G. Franz, H.D. Ables, C.C. Dahn, Lowell Observatory, Flagstaff, Ariz.), 199 (1987).
- "Naked eye star visibility and limiting magnitude mapped from DMSP-OLS satellite data" P. Cinzano, F. Falchi, C.D. Elvidge Monthly Notices of the Royal Astronomical Society, 323, 34–46 (2001)
- NOAA UK isophotic data for 1993 and 2000 (NOAA/ CPRE)
- "Parliamentary Science and Technology Committee report on light pollution and astronomy". HMSO. 2003
- "Scatter phase functions" From F Riewe and A ES Green Applied optics vol. 17 no 12 1978/June
- "The Artificial Sky Luminance And The Emission Angles Of The Upward Light Flux" P. Cinzano, F.J. Diaz Castro Measuring and Modelling Light Pollution, ed. P. Cinzano, vol.71, 251–256 (2000) – submitted May 1998
- "The first world atlas of the artificial night sky brightness" P. Cinzano, F. Falchi, C.D. Elvidge Monthly Notices of the Royal Astronomical Society, 328, 689-707 (2001)
- webexhibits.org <http://webexhibits.org/causesofcolor/14B.html>